

Distribution and origin of patterned ground on Mullins Valley debris-covered glacier, Antarctica: the roles of ice flow and sublimation

JOSEPH S. LEVY¹, DAVID R. MARCHANT² and JAMES W. HEAD III¹

¹Brown University, Department of Geological Sciences, Providence, RI, USA

²Boston University, Department of Earth Sciences, Boston, MA, USA

Abstract: We map polygonally patterned ground formed in sublimation tills that overlie debris-covered glaciers in Mullins Valley and central Beacon Valley, in southern Victoria Land, Antarctica, and distinguish five morphological zones. Where the Mullins Valley debris-covered glacier debouches into Beacon Valley, polygonal patterning transitions from radial (orthogonal) intersections to non-oriented (hexagonal) intersections, providing a time-series of polygon evolution within a single microclimate. We offer the following model for polygon formation and evolution in the Mullins Valley system. Near-vertical cracks that ultimately outline polygons are produced by thermal contraction in the glacier ice. Some of these cracks may initially be oriented radial to maximum surface velocities by pre-existing structural stresses and material weaknesses in the glacier ice. In areas of relatively rapid flow, polygons are oriented down-valley forming an overall fan pattern radial to maximum ice velocity. As glacier flow moves the cracks down-valley, minor variations in flow rate deform polygons, giving rise to deformed radial polygons. Non-oriented (largely hexagonal) polygons commonly form in regions of stagnant and/or near-stagnant ice. We propose that orientation and morphology of contraction-crack polygons in sublimation tills can thus be used as an indicator of rates of subsurface ice flow.

Received 7 October 2005, accepted 21 April 2006

Key words: Dry Valleys, ice rheology, polygon, soil-forming processes, sublimation till

Introduction

Polygonally patterned ground is a ubiquitous feature of the McMurdo Dry Valleys. Although classically described as networks of roughly hexagonal polygonal mounds and linear troughs (Péwé 1974), many polygon networks show a distinct preference in orientation, often associated with orthogonally intersecting troughs (Lachenbruch 1962, Abramenko & Kuzmin 2004, Mangold 2005). Polygons may have as few as three sides, defined by bounding troughs, but polygons with as many as eight sides occur in Mullins and Beacon valleys. The persistence of polygonally patterned ground in the Antarctic is a strong geological indicator of climate stability (Marchant & Head 2004, Marchant *et al.* 2002). Although the basic process of crack initiation and expansion due to seasonal-to-annual scale thermal contraction of frozen ground is well described (Lachenbruch 1962), the processes of polygon network modification and evolution are still being actively pursued (e.g. Mellon 1997, Marchant *et al.* 2002, Plug & Werner 2002, Sletten *et al.* 2003).

Of particular interest are the morphological and genetic differences in the development of ice-wedge polygons (in which seasonal meltwater fills and expands thermal contraction cracks), sand-wedge polygons (in which wind-blown aeolian material and loose surficial debris fill the thermal contraction cracks), and sublimation polygons (in which sublimation is the primary agent modifying thermal contraction cracks that form directly in buried ice)

(Marchant *et al.* 2002, Marchant & Head 2004). These species of polygons are geologically distinct entities and are the result of significantly different physical processes that produce highly variable morphologies (such as raised rims associated with ice-wedge polygons versus raised centres associated with sublimation polygons) (Marchant *et al.* 2002, Marchant & Head 2004, Sletten *et al.* 2003). Also of interest is the spatial distribution of polygonally patterned ground between large-scale climate zones (e.g. Arctic vs

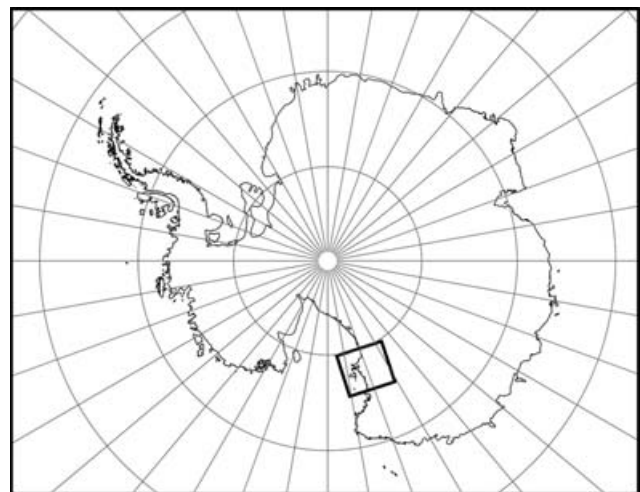


Fig. 1. Location map of Antarctica showing the McMurdo Dry Valleys (box).

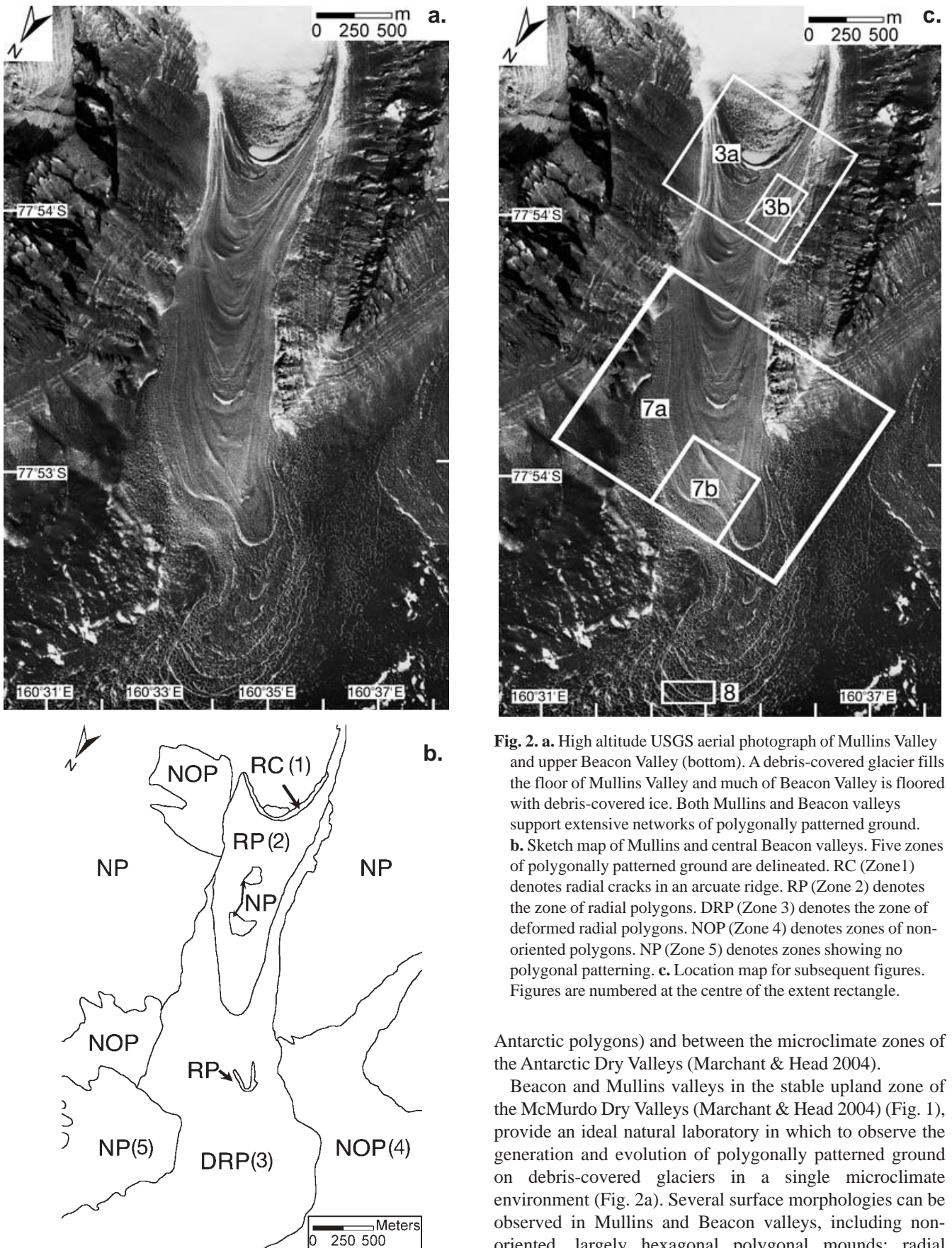


Fig. 2. **a.** High altitude USGS aerial photograph of Mullins Valley and upper Beacon Valley (bottom). A debris-covered glacier fills the floor of Mullins Valley and much of Beacon Valley is flooded with debris-covered ice. Both Mullins and Beacon valleys support extensive networks of polygonally patterned ground. **b.** Sketch map of Mullins and central Beacon valleys. Five zones of polygonally patterned ground are delineated. RC (Zone 1) denotes radial cracks in an arcuate ridge. RP (Zone 2) denotes the zone of radial polygons. DRP (Zone 3) denotes the zone of deformed radial polygons. NOP (Zone 4) denotes zones of non-oriented polygons. NP (Zone 5) denotes zones showing no polygonal patterning. **c.** Location map for subsequent figures. Figures are numbered at the centre of the extent rectangle.

Antarctic polygons) and between the microclimate zones of the Antarctic Dry Valleys (Marchant & Head 2004).

Beacon and Mullins valleys in the stable upland zone of the McMurdo Dry Valleys (Marchant & Head 2004) (Fig. 1), provide an ideal natural laboratory in which to observe the generation and evolution of polygonally patterned ground on debris-covered glaciers in a single microclimate environment (Fig. 2a). Several surface morphologies can be observed in Mullins and Beacon valleys, including non-oriented, largely hexagonal polygonal mounds; radial

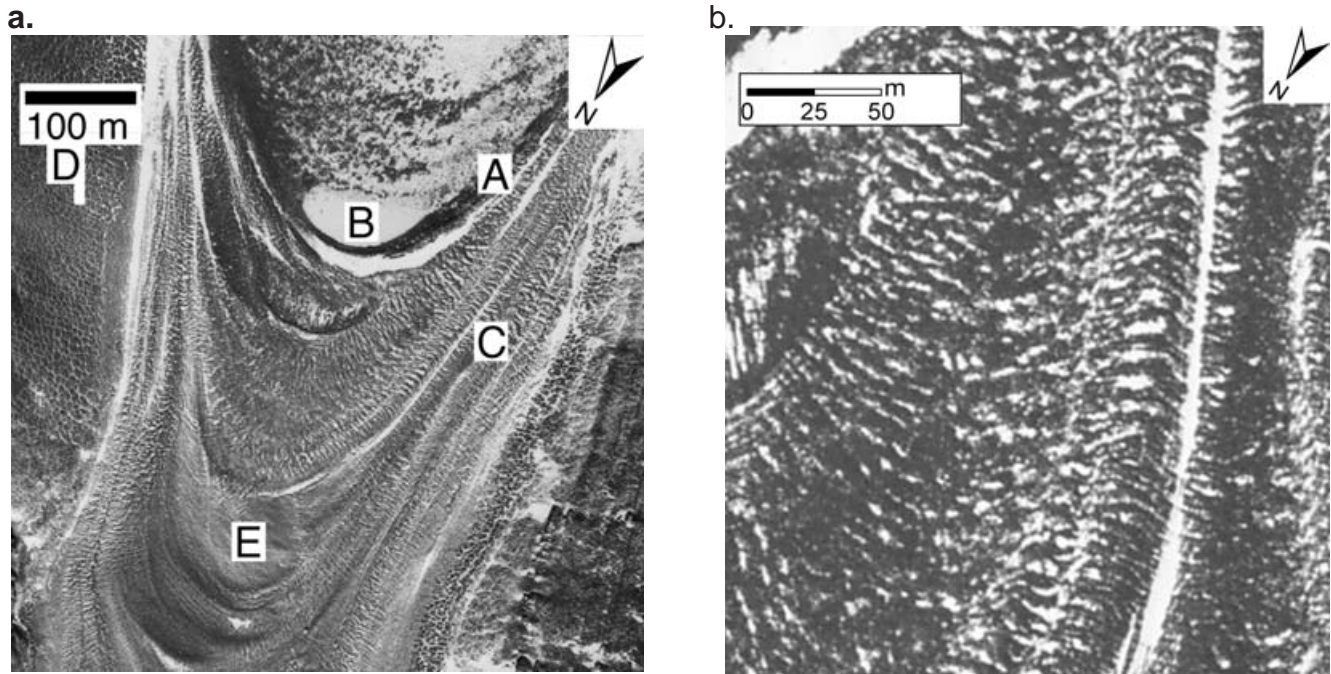


Fig. 3. a. High altitude aerial photograph showing lobes and polygons in upper Mullins Valley. The letter A marks a ridge in which radial cracks in ice (see Fig. 5) are present; B marks a perennially frozen pond produced from minor, albedo-controlled surface melting; C, radial polygons; D, the northern wall of Mullins Valley, which exhibits non-oriented polygons; and E an area where no polygons are visible. Down-valley is to image bottom. **b.** Cambot high-resolution image of radial polygons in upper Mullins Valley. Radial cracks are visible both at the front of the glacial sub-lobe, as well as on the lobe interior. Curving troughs which follow the arc of the lobe orthogonally transect the radial troughs. Down-valley is to image bottom.

polygons with orthogonally intersecting troughs; areas in which no polygons are present; and zones in which radial cracks are present, but which have not been modified into fully expressed polygons. We have mapped these surface

morphologies in Mullins Valley and the nearest reaches of Beacon Valley using high-resolution air photographs, as well as field mapping, and present a description of the surface and underlying characteristics of these morphological units

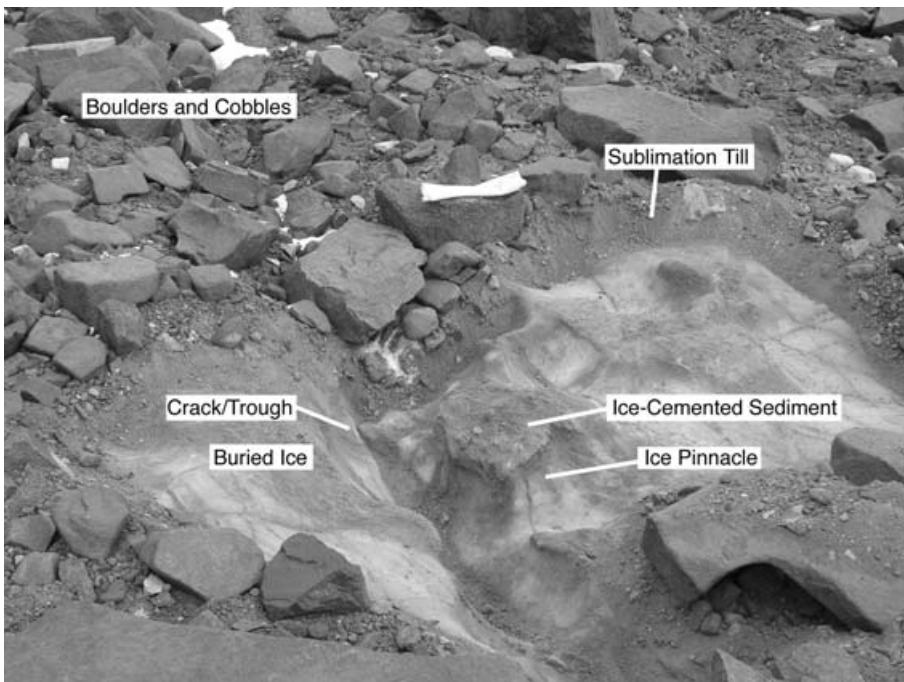


Fig. 4. Excavation in Mullins Valley. The till sequence above the debris-covered glacier is clearly discernable: buried glacier ice beneath a thin layer of ice-cemented sediment and overlying dry sublimation till. A ~30 cm wide, folded, white sample bag is included for scale (upper centre).

(Fig. 2b). This work builds on early quantitative morphological studies of Mullins and central Beacon valleys that focused on changes in polygon trough morphology exclusively as a function of distance down-valley (Lorrey 2002), adding descriptions of the relationships between surface units observed in the valleys. We do not define the morphological units as a function of distance down-valley. Rather, we trace morphology by focusing on the sub-lobe structures which dominate the surface of the Mullins Valley debris-covered glacier.

Description of Mullins Valley field site

Mullins Valley (77°54'S, 160°35'E) is a tributary to Beacon Valley (77°49'S, 160°39'E) and is located in the stable upland zone of the McMurdo Dry Valleys (Marchant & Head 2004). Climatically, Mullins Valley is hyper-arid, with an annual water equivalent precipitation of $< 10 \text{ mm yr}^{-1}$ (Schwerdtfeger 1984). Air temperatures range from a winter minimum of -48°C (Doran *et al.* 1995) to a summer maximum of $\sim +3^\circ\text{C}$ (Kowalewski *et al.* 2006). Mean annual temperature on the floor of central Beacon Valley

($\sim 100 \text{ m}$ below the head of Mullins valley) is around -22°C (Doran *et al.* 1995).

The floor of Mullins Valley is dominated by Mullins glacier, a debris-covered glacier at least 6 km long and 0.8 km wide (Fig. 2a). The surface of the glacier shows several distinct lobes that are nested axially down-valley (Fig. 3a). We map five distinct morphological units on Mullins glacier (Fig. 2b):

Zone 1: Radial crack formation (RC).

Zone 2: Radial polygons (RP).

Zone 3: Deformed radial polygons (DRP).

Zone 4: Non-oriented (“hexagonal”) polygons (NOP).

Zone 5: No polygons (NP).

The near-surface sequence of sublimation tills that cap debris-covered glacier ice in Beacon Valley is well described by Sugden *et al.* (1995) and Marchant *et al.* (2002) (Fig. 4). The till sequence changes markedly across polygons, with sediment at polygon centres largely reflecting the passive accumulation of till as debris-rich ice sublimates and the sediment at polygon troughs reflecting a

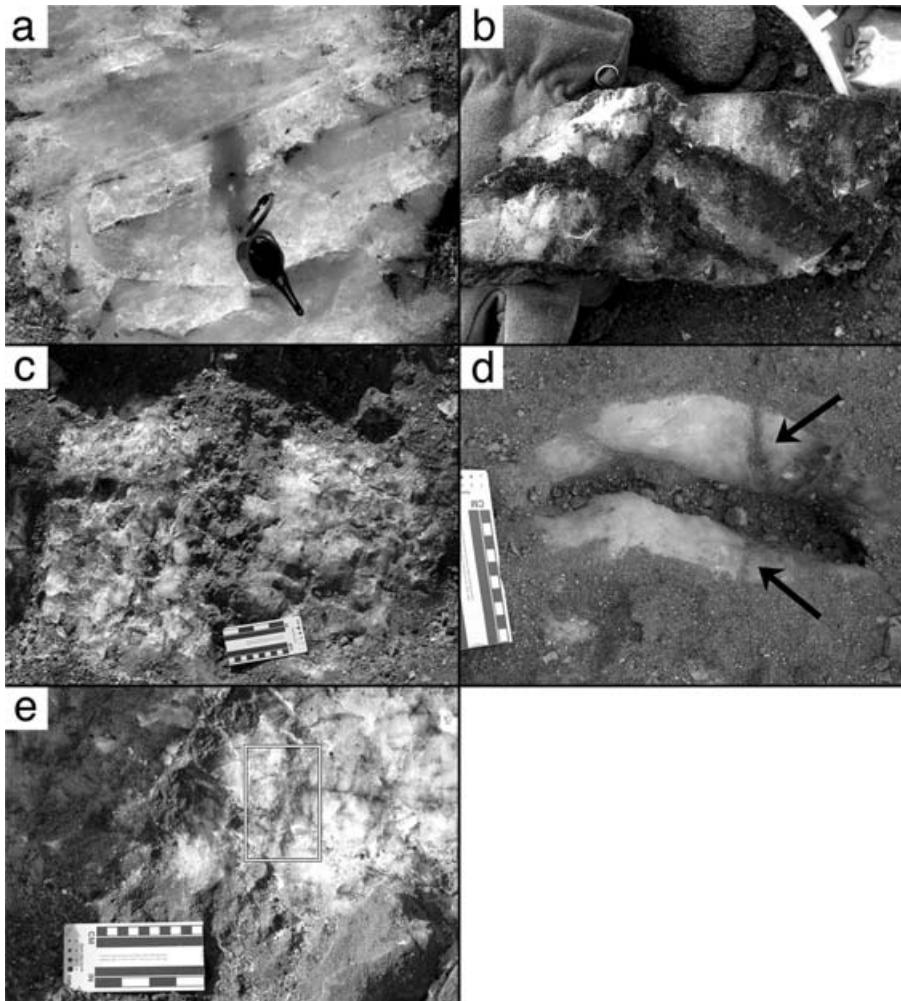


Fig. 5. Crack morphologies observed in plan-view in the most prominent arcuate ridge in upper Mullins Valley (labelled A in Fig. 3). Photographs have been contrast-adjusted to enhance clarity. **a.** Simple fractures in the ice with no fill material. **b.** Detached block of ice cut away from buried glacier showing sand-filled cracks $\sim 1 \text{ cm}$ wide, some intersecting at angles close to 90° . **c.** A 3-cm wide crack filled with ice-cemented sands and small gravel-sized clasts trending up and down at image centre. **d.** Loose-sand-filled crack with several smaller cracks intersecting at angles close to 90° (arrows). Note that crack widening near the glacier surface indicates loss of adjacent glacier ice by sublimation. **e.** Composite crack, boxed, in which vertically laminated, ice-cemented sands surround an inner vertical band of ice parallel to crack orientation.

combination of aeolian infill, slumped debris, and winnowed till (Marchant *et al.* 2002). For polygon troughs, the following sequence is commonly observed: resting above the ice is a patchy layer of ice-cemented sediments and winnowed till. This ice-cemented till ranges from a few mm to several centimetres in thickness. Above this ice-cemented sediment layer is a collection of dry and winnowed sublimation till up to 1 m in thickness (but commonly only tens of centimetres thick) composed of doleritic sand, pebbles, and cobble-sized material. The winnowed sublimation lag grades upward into a zone of weathered dolerite and sandstone material, ranging in size from sub-mm to 50 cm scale or larger. This material armors the loose, underlying sands and prevents extensive aeolian deflation. The largest troughs trap windblown snow, producing perennial snowbanks that help delineate polygon boundaries. The present ground topography generally follows the surface of the buried ice. However, ice pinnacles and ice-cemented sediment pinnacles without surface expressions are developed at the margins of some polygon troughs. Additionally, local depressions of the ice surface may occur beneath large surface boulders.

Zone 1: Radial crack formation (RC)

A large, arcuate ridge, ranging from 8–30 m wide, 6 m high, and 880 m long, (convex down-valley) marks the area of



Fig. 6. A snow bank (foreground) in a topographic low between glacial lobes into which radial polygons terminate (Zone 2, RP). The flaring of the polygon trough at the snow bank is interpreted as a result of enhanced sublimation at the break in slope (which allows both vertical and horizontal diffusion of water vapour). A portion of the accumulation zone for Mullins Valley debris-covered glacier at the valley head can be seen in the background.

observed nascent crack formation in Mullins Valley (Fig. 2b, RC; Fig. 3a). Fourteen excavations were made into the summit, flanks, and base in order to expose the ice substrate. The average depth to ice beneath sublimation till for these excavations was ~4.5 cm, with a range of 2–10 cm. The buried ice is commonly cracked, and the bearing (000°–180°) of each crack was measured. The main cracks are largely normal to the ridge-front, forming a radial suite ranging from 000° to 180°, distributed appropriately around the curvature of the ridge.

Several crack morphologies are developed in the ice-cored ridge (Fig. 5). Simple fractures in the ice with no fill material are very common and are approximately 1 mm wide, but may be centimetres to tens of centimetres long. Cracks filled with loose sand are about as common as those without fill material and range in width from mm-scale to cm-scale. Cracks filled with ice-cemented sand are also present and range in width from mm-scale to 3 cm, with the widest ranging up to 7 cm. The ice-cemented sands in these cracks are commonly laminated, showing vertical layering parallel to crack orientation. Some cracks are observed in which vertically laminated, cemented sand material flanks a central, vertical band of ice, which also runs parallel to crack orientation. The width of such cracks range from 1–3 cm, with the central ice band being < 1 cm wide.

Cracks in the ice occur throughout the ridge, with no changes in crack density associated with position on the ridge (e.g. flank, crest, base, area of maximum curvature, etc.). Cracks commonly occur sub-parallel within a single soil excavation, but intersecting cracks also occur. Some large cracks, particularly those filled with ice-cemented material, are associated with smaller cracks that branch off at angles ranging from 70–90° from the large crack.

Zone 2: Radial polygons (RP)

Down-valley from the zone of radial crack formation, polygonal troughs and mounds dominate the surface morphology of the sublimation till. Troughs and intervening mounds are generally radial about the lobe on which they form (Fig. 3a & b, Fig. 6) The polygonal mounds are metres to tens of metres long, up to 3 m wide, and are commonly segmented by small troughs cutting orthogonally across the long axis. The polygons are generally tetragonal and up to a metre of relief is common between the mound crest and snow that collects in polygon troughs. Sublimation till in this zone averages ~7 cm thick, with a range of 3–10 cm. Till may overlie patchy ice-cemented layers ~3 cm in thickness. The radial orientation of the polygon network, as well as the orthogonal intersection of troughs, is most apparent near the margins of prominent surface lobes; however, radial patterning is observed well into the centres of the most up-valley lobes within this morphological unit.

The termini of many radial polygons are conformable with a continuous snow bank that occupies a topographic

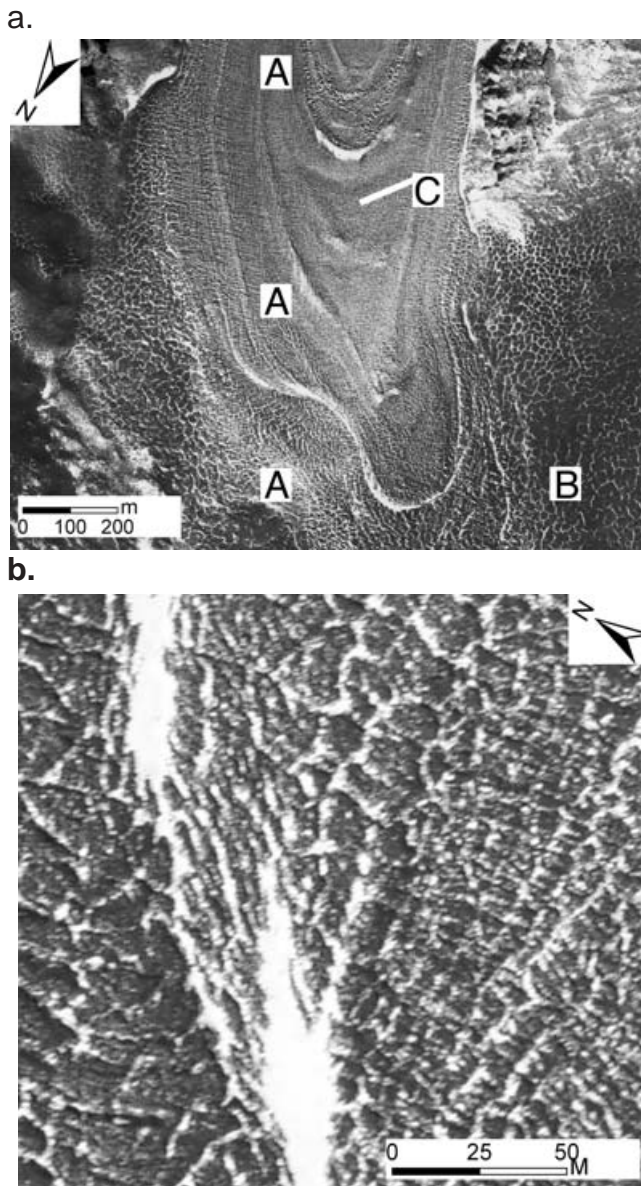


Fig. 7. a. High altitude air photograph of lower Mullins Valley. Letter A marks deformed radial polygons; B, an area of non-oriented polygons; C, an area with no polygonal patterning. Down-valley is to image bottom. **b.** Cambot high-resolution image of deformed radial polygons in lower Mullins Valley (see Fig. 2c). Although the polygons are still delimited by largely orthogonal troughs, many polygons show evidence of deformation, including bending of troughs and the development of additional, non-orthogonal bounding troughs.

low between glacial lobes. At this boundary, the widths of the polygon troughs expand from a few tens of centimetres to a metre or more, producing triangular terminal flares in the troughs and tapering of the polygon mounds (Fig. 6).

In excavations across the tapering polygon mounds, the surficial till and debris-cover is up to ~14 cm deep. The base of the till commonly contains a layer of ice-cemented sand and pebbles, 2–4 cm thick, and the underlying glacier ice is crosscut with multiple intersecting sand-filled cracks.

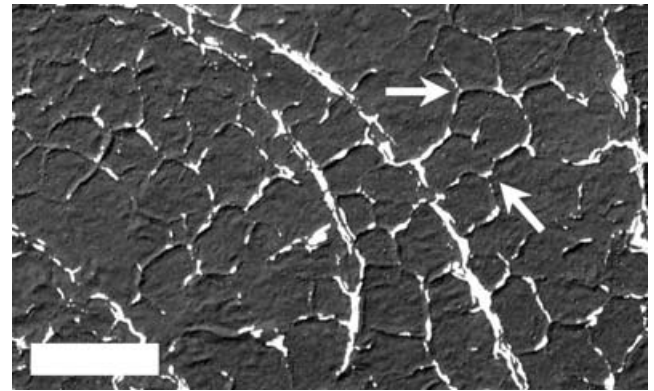


Fig. 8. Cambot image of non-oriented polygons at the junction of Mullins and Beacon valleys. Polygons are defined by largely hexagonal intersections (as indicated by arrows). Scale bar is approximately 30 m in length.

The terminal flares at the end of radial polygon troughs have a strikingly different morphology from that of adjacent polygon mounds. In the terminal flares, till thickness increases substantially, reaching up to ~24 cm, with an average thickness of 8–10 cm. The axis of the polygon trough is observable as a sand- or sand and ice-filled crack, commonly ~3 cm in width, with abundant finer cracks crossing the main crack at angles approaching 90°.

Zone 3: Deformed radial polygons (DRP)

Zone 2 (radial polygons) grades into Zone 3 (deformed radial polygons) in which polygonal structure is less clearly oriented. Deformed radial polygons are particularly apparent along the lateral margins of the Mullins Valley debris-covered glacier and near its confluence with Beacon Valley (Fig. 2, DRP; Fig. 7). Zones of deformed radial polygons often separate zones of clearly defined radial polygons from areas showing polygonal patterning with no preferred orientation (Fig. 7). Many of the deformed radial polygons are largely tetragonal, with predominantly orthogonal intersections between polygon troughs. Some polygons have additional faces (up to 5 or 6) defined by troughs that have either formed at non-right angles, or which have been subsequently deformed into non-orthogonal intersections.

Deformed radial polygons were excavated to examine the morphological effects of active and inactive troughs on polygon mound morphology (in active troughs, recent thermal cracking may be observed indirectly through the settling of sand grains into the wedge, resulting in a paucity of sand material covering the crack). We excavated a conical polygon mound approximately 4 m wide and 2 m in relief, surrounded by active troughs on three of four sides and a subdued trough on the north-facing margin. The mound is covered with 20–50 cm scale cobbles and boulders of dolerite and sandstone, which transition downward into a 30 cm thick layer of clasts and sand material (dominated and supported by the cobbles). 20–50 cm below

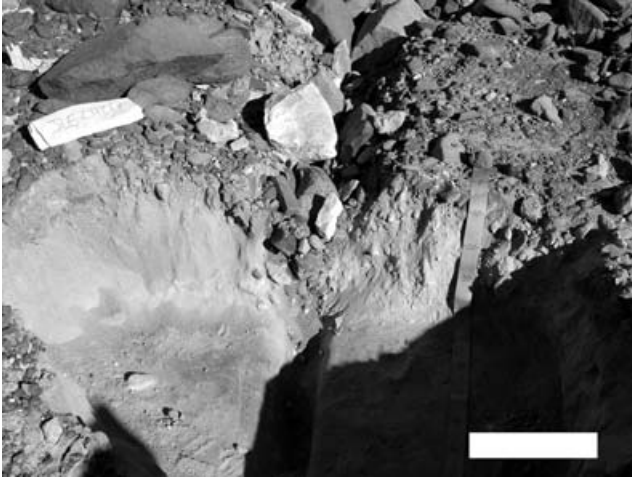


Fig. 9. Excavation across a relatively small thermal-contraction-crack trough in sublimation till over buried ice in central Beacon Valley. The trough extends down into the buried ice and near the surface it has been widened by differential sublimation. The white scale bar is 40 cm long.

this layer, the polygon is cored with glacier ice. The contact between the sands and the underlying ice is smooth, without physical evidence for subsurface melting and/or ice-cemented sands. A truncated relict wedge runs north-east from the polygon margin to the polygon centre.

Zone 4: Non-oriented polygons (NOP)

In upper Beacon Valley and the lowest reaches of Mullins

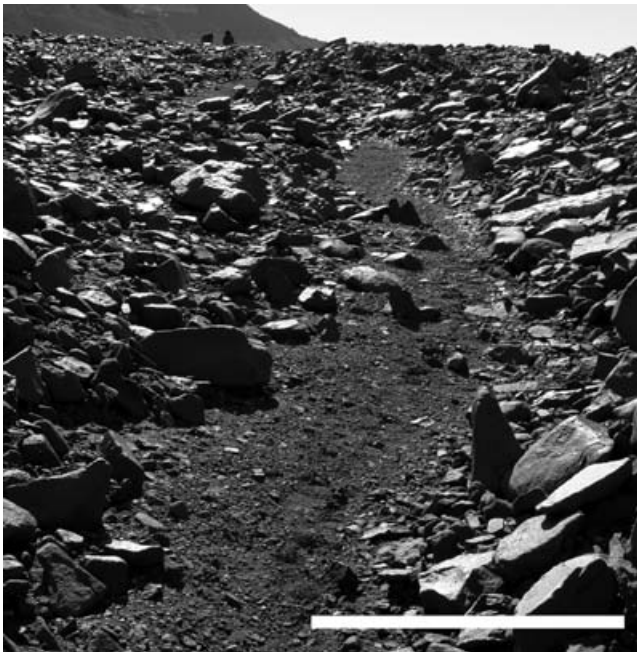


Fig. 10. A mature polygon trough in central Beacon Valley. Scale bar is approximately 1 m long.

Valley, non-oriented, largely hexagonal polygons are present (Fig. 2, NOP; Fig. 8). There are several general morphological classes of polygons in this zone. Raised-centre, sublimation-type polygons defined by small bounding troughs and showing no more than 1 m of vertical relief between the observable base of the trough and the crest of the polygon mound are common. Also present are higher-relief polygons with 4–8 distinct sides and 1–3 m of relief from the base of the trough to the polygon mound crest. Some polygon mounds are nearly round, without distinctly intersecting linear troughs, and are surrounded by a depressed moat, resulting in a hummocky appearance. These polygons range in relief from 1–5 m from the base of the trough to the mound crest. It is possible that this suite of non-oriented polygons represents a maturation sequence as thermal contraction cracks form and evolve, and as surrounding ice is lost by differential sublimation.

Polygon troughs on the valley floors are variable in size and activity (Figs 9 & 10). The smallest polygon troughs are little more than locations where cracks have formed in the underlying ice, leading to local trapping of fine-grained



Fig. 11. The intersection of two thermal contraction cracks in the centre of a polygon mound located in central Beacon Valley. The crack oriented to the right is interpreted to be younger than the transverse crack due to its smaller size and orthogonal intersection with the larger crack (after Lachenbruch 1962). The scale bar (upper left corner) is 50 cm in length.

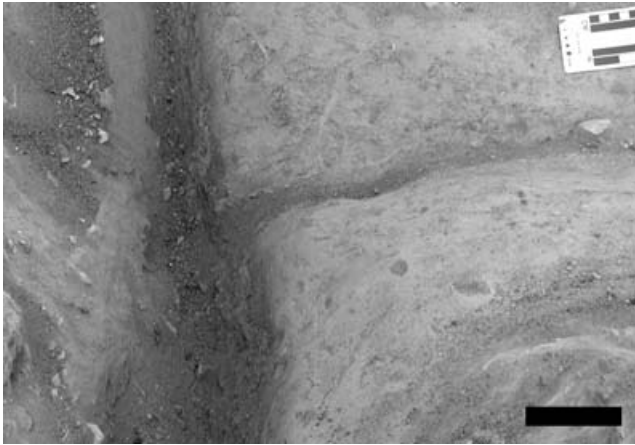


Fig. 12. Close-up view of the orthogonal crack intersection featured in Fig. 11. The smaller (and most likely younger) crack widens towards the intersection with the larger crack. This pattern is similar to the flaring observed at the intersection of radial polygon troughs and the bounding snow banks in Zone 2 (RC) (see also Fig. 6). Both phenomena are interpreted to be a result of enhanced sublimation in the vicinity of crack intersection. A black scale bar (lower right) is 10 cm in length.

material, largely from the downward percolation of overlying, dry till. These cracks may be manifest on the surface as a thin furrow several cm wide. Larger troughs show signs of significant modification due to sublimation of adjacent glacier ice (Marchant *et al.* 2002), resulting in widening of the trough and the concentration of larger cobbles and small boulders in the trough (which are too large to enter the crack itself). The largest active troughs are filled with boulder-sized material, slumped from trough walls, making excavation extremely difficult. The largest active troughs are several metres wide. Inactive, relict troughs (representing locations of former polygon boundaries) bound some polygon mounds or are present in mound interiors, cross-cut by active troughs. These relict troughs show little relief and are distinguished at the ground surface by the observation of linear accumulations of sandy material. Relict troughs may range in width from a few tens of centimetres to several metres. The largest such troughs may contain a zone of surface boulders that reflect accumulation via slumping along steep walls when the trough was active. Some of these relict troughs may contain deposits of *in situ* ashfall as much as 8.1 million years old (Ma) (Sugden *et al.* 1995, Marchant *et al.* 1996)

Intersection angles between active polygon troughs in Zone 4 (NOP) are quite variable. Both near-orthogonal and near-hexagonal intersections are developed. The smallest troughs, which are interpreted to result from the youngest cracks, are largely orthogonal, propagating into or out of pre-existing troughs (Figs 11 & 12). Where smaller troughs intersect larger polygon troughs, usually the result of the propagation of a crack between the polygon centre and a

bounding polygon trough, there is some widening of the smaller trough in the vicinity of the intersection (Figs 11 & 12). This morphology is similar to the terminal flaring observed when polygon troughs intersect the bounding snow banks in Zone 2 (RP). Some of these expanded troughs are filled with deep sand, 1 m or more in thickness, as well as large boulders that may have slid down from oversteepened trough walls.

Zone 5: No polygons (NP)

Within the central stretches of the Mullins Valley debris-covered glacier and in certain regions of Beacon Valley the surface lacks polygons (Fig. 2, NP; Fig. 7a). These areas have ground cover similar to those areas featuring polygons, including a sandy subsurface lag overlain by cobble and boulder-sized fragments of weathered dolerite and sandstone. The surface is relatively smooth with a pavement formed of interlocking cobbles. Contacts between regions with no polygons and polygonally patterned ground are gradational, with small troughs extending out of the polygon-free zone into polygonally patterned areas.

In order to contrast polygon morphology on the Mullins Valley debris-covered glacier with polygon morphology on a non-glacial surface, excavations into the walls of Mullins Valley (where no glacial ice is present) were made. Ice-cemented colluvium is present on the valley walls; no massive ice was observed. Polygon troughs on the north wall are easily distinguished in air photos and on the ground by the presence of perennial snow banks in polygon troughs (Fig. 2a). The rock cover is dominated by dolerite cobbles above coarse sand with very few fines. The sandy material is cemented with interstitial ice from 2–15 cm depth and in places overlies ice with sporadic cobbles up to 10 cm in scale, and numerous sand veins.

Trough intersection angles

In order to quantify differences between the morphological units mapped in Mullins and Beacon valleys, the angles of 198 polygon trough intersections were measured in zones 2 (RP), 3 (DRP), and 4 (NOP) (Table I). The smallest angle between adjacent troughs was measured using georeferenced air photographs, resulting in measurements between 0–90°. For Mullins Valley, trough intersections were measured only where snow banks could be used to

Table I. Polygon trough intersection angle by zone.

Morphological zone	Low-angle intersection (10–39°)	Near- hexagonal (40–79°)	Near- orthogonal (80–90°)
Zone 2 (Radial Polygons, RP)	0%	44%	56%
Zone 3 (Deformed Radial Polygons, DRP)	10%	56%	34%
Zone 4 (Non-Oriented Polygons, NOP)	6%	77%	17%

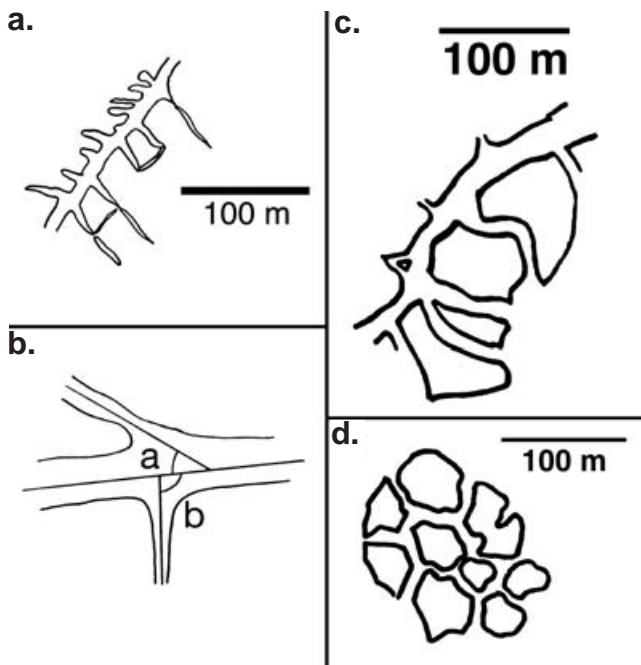


Fig. 13. Schematic diagrams of polygon mound and trough morphologies in map view. Sketches are generalized from air-photograph data. **a.** Typical polygon troughs in Zone 2 (RP). Three-element intersections dominate the largely orthogonal intersections in this zone. **b.** Schematic of trough intersection angle measurements with no particular scale. Angle-a marks a low-angle intersection. Only angles 0–90° were measured, as obtuse angles can be simplified to acute angles for analysis. Angle-b marks a near-orthogonal intersection. **c.** Example showing polygons in Zone 3 (DRP) with near-orthogonal, near-hexagonal, and low-angle intersections. **d.** Schematic morphologies in Zone 4 (NOP). These polygons are largely hexagonal with nearly straight troughs that have been modified by sublimation of adjacent ice, creating oversteepened trough walls that ultimately fail by infrequent and slumping. On the basis of cosmogenic-nuclide data, Marchant *et al.* (2002) estimated the time interval since slumping along the margin of two polygon troughs in central Beacon Valley to be 1.18 million years and 0.18 million years.

clearly delineate the intersecting troughs.

Zone 2 (radial polygons) is dominated (56%) by near-orthogonal trough intersection angles (80–90°), reflecting the strongly orthogonal character of the trough intersections apparent from inspection. Near-hexagonal (40–79°) intersections account for the remaining intersections (44%). Although classic hexagonal polygons are dominated by near-60° trough intersections, inspection of this zone indicates that the majority of these lower-angle intersections are associated with roughly tetragonal polygon mounds (Fig. 3). The trough intersections measured were predominately located along the curving snow bank, which defines the margin of the zone, resulting in an abundance of three-way “T-intersections” and very few four-way

intersections. This accounts for the absence of low angle (10–39°) intersections, which might otherwise be expected in a zone of orthogonally intersecting polygon troughs, as low angle intersections (10–39°) are commonly indicative of near-orthogonal intersections where two troughs cross, or where proximal, but unrelated intersections occur, producing a four-way intersection (Fig. 13).

Zone 3 (deformed radial polygons) contains three distinct populations of trough intersections. Near-hexagonal (40–79°) intersections are most abundant (56%), followed by near-orthogonal (80–90°) intersections (34%). A small cluster of low-angle (10–39°) intersections is also present, accounting for 10% of measured intersections.

Zone 4 (non-oriented polygons) contains a modal distribution of trough intersections. Near-hexagonal (40–79°) intersections dominate the distribution (77%), followed in abundance by near-orthogonal (80–90°) intersections (17%), and a small population of low-angle (10–39°) intersections (6%).

Polygon morphology and ice flow rates

Calculations of horizontal ice flow for the debris-covered glacier ice in Mullins and Beacon valleys provide an invaluable test of the influence of glacial deformation on polygon morphology. Rignot *et al.* (2002) measured surface displacement of the Mullins Valley debris-covered glacier using synthetic-aperture radar interferometry (InSAR). Their combined InSAR and glacial modeling results show that

- 1) horizontal surface velocities decrease down glacier, from a maximum of ~ 40 mm in the accumulation zone to as low as ~ < 1 mm on the floor of upper Beacon Valley, and
- 2) measurements of surface displacement delineate zones that are spatially comparable with mapped surface lobes on the Mullins Valley debris-covered glacier.

In addition, zones of relatively high- and low-velocity surface displacement as inferred from InSAR in Rignot *et al.* (2002) appear spatially consistent with our mapped zones of polygon morphology. Zones of relatively high surface velocities display radial polygons (RP); zones of relatively low surface velocity that occur just down-glacier from local velocity maxima display deformed radial polygons (DRP) (possibly indicating previous deformation which has largely ceased at the present time) and non-oriented polygons (NOP). These observations are consistent with the hypothesis that radial polygons are predominantly a product of thermal contraction crack formation in a pre-existing extensional stress field oriented by glacial flow. Further, areas subject to slower surface flow rates experience less dramatic extensional stress, resulting in the formation of loosely oriented radial polygons. Areas underlain by stagnant glacial ice experience no orientation

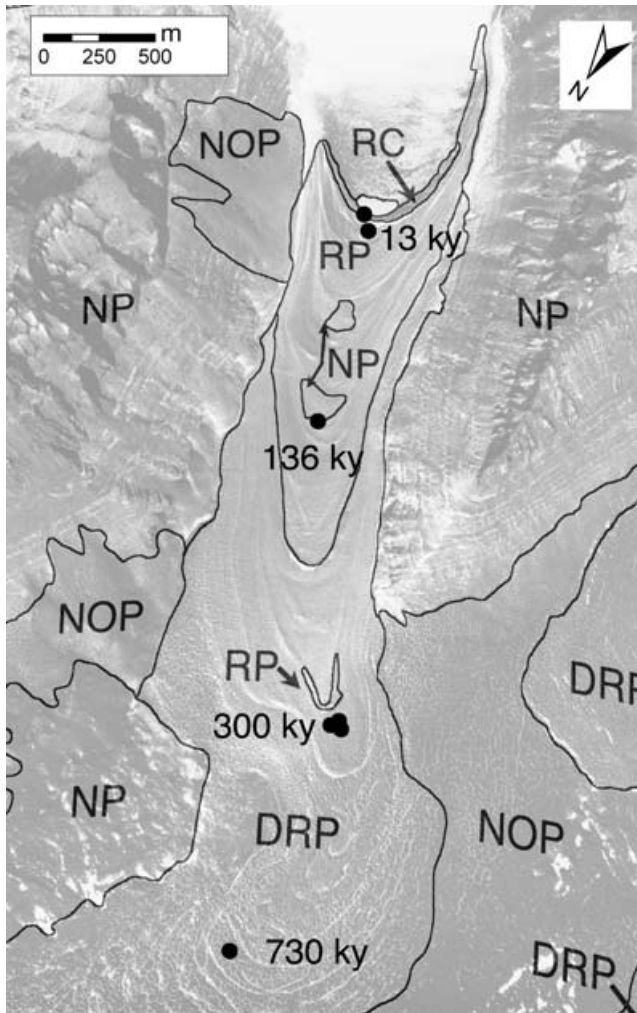


Fig. 14. Overlay of the Mullins and central Beacon valleys polygon morphology sketch map onto high resolution image data. Preliminary cosmogenic nuclide exposure ages (Schaeffer *et al.* 2005) are marked adjacent to dark circles which denote the approximate location of sample collection. Ages increase dramatically down valley.

of the local stress field, resulting in the formation of classically described hexagonal polygons.

Cosmogenic nuclide exposure ages

As the Mullins Valley debris-covered glacier flows down-valley, englacial debris is brought to the ice surface along a curving trajectory by the sublimation of overlying ice. The accumulated debris forms a sublimation lag or till (e.g. McCall 1960) that retards further ice loss. Given that surface rocks are continually transported down-valley, and are exposed to high-energy cosmic rays; the measured concentration of *in situ* produced cosmogenic nuclides in these surface rocks can be used to estimate till age and, indirectly, minimum ages for the ice below (Schaefer 2000).

Schaefer *et al.* (2005) reported preliminary He-3

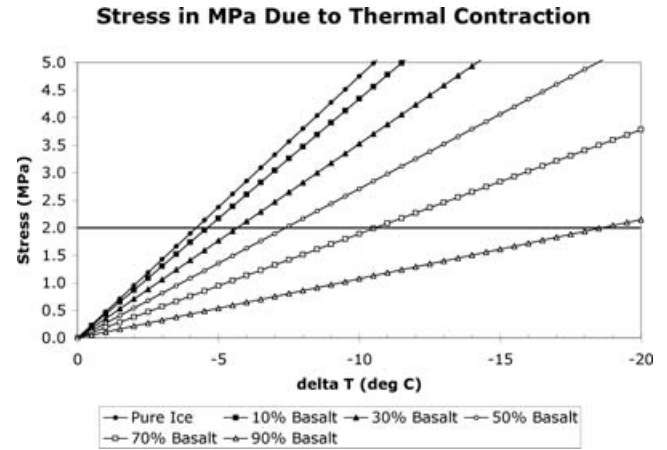


Fig. 15. Results from an elementary elastic stress model for pure ice, assuming the only stress is thermal contraction of an elastic medium. Stresses exceeding 2 MPa (the threshold value for crack formation in ice, e.g. Mellon 1997) are easily attained with temperature variations as little as 4°C.

cosmogenic-nuclide ages for surface cobbles sampled along a transect down the axis of the Mullins Valley debris-covered glacier (Fig. 14). Ages increase from ~13 ka near the valley head to as much as 730 ka in upper Beacon Valley. Assuming limited nuclide inheritance (a reasonable assumption given the 13 ka age near the head of Mullins Valley), these preliminary cosmogenic results suggest a decrease in the rate of ice flow down valley and appear consistent with the reported surface displacements as deduced from InSAR (Rignot *et al.* 2002). These data may also be used to help estimate polygon longevity (see below).

Thermal stress in pure ice

To evaluate the origin of stress that leads to polygonal cracking, we attempt to constrain the magnitude of stresses that can be generated in the Dry Valleys. Conservatively, thermal stresses must be in excess of 2 MPa to generate contraction cracks in pure ice (Mellon 1997). Using a simple, purely elastic model, we ascertain that, assuming a fairly well-coupled air-temperature/ground-temperature relationship in Mullins and Beacon valleys (Doran *et al.* 1995), thermal contraction due to seasonal temperature change is adequate to overcome the 2 MPa threshold for thermal contraction cracking (Fig. 15).

Employing a first order elastic stress relation:

$$-\alpha(\Delta T)E = \sigma \quad (1)$$

where α is the coefficient of thermal expansion of pure ice (5×10^{-5}), ΔT is temperature change from mean annual temperature in °C, E is Young's modulus for pure ice ($\sim 9.5 \times 10^9$ Pa), and σ is stress in Pa, assuming a positive stress magnitude is tensile in nature (values are conservative averages drawn from Hobbs 1974). Thus, in a purely elastic regime, a temperature change of only -4.2°C below the

mean annual temperature should be adequate to generate thermal contraction cracks. Air temperature variation of this magnitude occurs every year in Mullins and Beacon valleys, suggesting that thermal contraction crack formation occurs annually (Doran *et al.* 1995, Marchant *et al.* 2002). However, it is likely that subsurface temperatures and the rate of subsurface temperature changes are moderated by the accumulation and distribution of sublimation till (Marchant *et al.* 2002). A more complete account of subsurface temperature conditions can be found in Kowalewski *et al.* (2006).

Discussion and interpretation

Much of the variation in polygon morphology on the Mullins Valley debris-covered glacier arises from interactions of glacier flow and modification of thermal contraction cracks by sublimation of adjacent ice.

The radially oriented cracks in Zone 1 (RC) are interpreted as thermal contraction cracks that form in an oriented, extensional stress-field produced by relatively rapid glacier flow along the front of a surface lobe. Thermal contraction overcomes the tensile strength of the buried ice, leading to cracking parallel to the direction of ice flow. Such cracking produces an arcuate array of contraction cracks along the arcuate lobe front, as tensional stresses associated with lobe expansion are oriented normal to the lobe front (Fig. 5). The largest of these cracks fill with sediment or ice-cemented sediment by the settling of fines from overlying till, producing morphologies similar to thermal contraction sand-wedge polygons. Smaller cracks may reseal. Cracks most likely originate at the buried ice surface, not within the overlying till, as the loose sandy till lacks sufficient cohesion to fail by thermal fracture.

The transition from Zone 1 (RC) to Zone 2 (RP) is interpreted as a maturation of cracks formed in Zone 1 due to sublimation of surrounding glacier ice and glacial flow. As glacial ice advances down-valley, pre-existing radial crack termini act as natural stress accumulators (e.g. Lachenbruch 1962). Continued glacier flow and yearly thermal contraction combine to propagate cracks into the interior of mapped surface lobes, as thermal contraction will tend to be focused at sites of pre-existing thermal contraction cracks (Lachenbruch 1962). As thermal contraction cracks mature into radial polygon troughs, sublimation acts to remove adjacent buried ice, resulting in a widening of the crack/trough into the v-shape characteristic of thermally-derived sublimation polygons (Marchant *et al.* 2002). This deepens the troughs, creating sheltering relief in which perennial snow banks can accumulate, and which may provide a negative feedback that slows further ice loss via sublimation (Marchant *et al.* 2002, Kowalewski *et al.* 2006).

Trough intersection-angle measurements shed considerable light on the evolution of radial polygons from

Zone 2 into deformed radial polygons in Zone 3. An internally consistent explanation that fits available data is as follows: near-orthogonal trough intersections (80–90°) in Zone 3 (DRP) reflect inheritance of radial polygon troughs generated in Zone 2 and transported down-valley by glacier flow. Near-hexagonal trough intersections (40–79°) in Zone 3 (DRP) reflect deformation of near-orthogonal trough intersections inherited from Zone 2, in addition to some hexagonal cracking in response to thermal stresses experienced during the duration of down-valley transport. Low-angle intersections (10–39°) in Zone 3 (DRP) reflect a lesser degree of deformation as a result of glacier flow (Fig. 13) or the abundance of new troughs that typically intersect and cross-cut pre-existing troughs at right angles (e.g. Lachenbruch 1962).

In Zone 4 (NOP) the abundance of near-hexagonal trough intersections (40–79°) is interpreted as a signature of thermal contraction crack formation in ice lacking an oriented tensile stress field generated by glacier flow. The intersection of a younger trough with a preexisting trough produces near-orthogonal intersections as originally suggested by Lachenbruch (1962) and illustrated in Figs 11 & 12. The paucity of deep and wide orthogonal intersection troughs in Zone 4 (NOP) suggests that few if any orthogonal intersection troughs that originated in Zones 2 and 3 moved down-valley to Zone 4 as a result of glacier flow. The minimum duration of the oldest orthogonal intersection polygons can be estimated by subtracting the inferred age of the sublimation till and polygons in Zone 3 (DRP) (which must be younger than Zone 4 polygons) from those of Zone 2 (RP): ~600 ky (Fig. 14).

Portions of Mullins Valley that show no polygonal patterning (Zone 5) are interpreted as areas in which either stresses have not accumulated adequately to produce thermal-contraction cracking, cracks have subsequently resealed as a consequence of glacial flow and vapour transport, or cracks have not matured sufficiently to be detectable at the ground surface. These areas are found largely within lobe interiors and are spatially correlated with regions analysed using InSAR as showing low range displacements (Rignot *et al.* 2002).

Combining the individual interpretations of each morphological zone, we can develop an integrated model to describe polygon growth and evolution on the Mullins Valley debris-covered glacier. Thermal contraction cracks initially form radial to the advancing glacier lobe (Zone 1) and mature into radially-oriented polygons characterized by orthogonal-intersection troughs (Zone 2). These radially oriented polygons (Zone 2) are transported surficially down-valley by glacial flow and undergo deformation related to variations in surface-ice velocity (Zone 3). Any orthogonal-intersection troughs inherited by glacier flow from Zones 1 and 2 apparently reseal by the time the surface has been transported out of Zone 3 and into upper Beacon Valley, as reflected by the lack of well-developed

orthogonal-intersection polygons in Zone 4. Resealing of orthogonal-intersection troughs results in the removal of inherited sites of material weakness (e.g. Lachenbruch 1962), which, combined with the lack of orienting stress from glacial flow, produces principally hexagonal, non-oriented polygons in Zone 4 (in response to annual thermal contraction).

Although this model is strongly suggested by the morphological evidence acquired in Mullins and Beacon valleys, several significant questions remain. First, when considering the formation of non-oriented hexagonal polygons in Zone 4 (NOP), how much tensile strength is added to the buried ice surface by the sealing of inactive polygon troughs? It seems likely that a sealed crack/trough must have a tensile strength equal to or greater than the tensile strength of uncracked, debris-covered ice; otherwise the existing trough would reactivate in response to subsequent thermal contraction (e.g. Lachenbruch 1962). Additionally, unless the tensile strength of the buried glacial ice is spatially uniform, cracks should reflect the positions of inherited orthogonal-intersection troughs or debris layers within the ice itself. Answers may come from a better understanding of changes in the thermo-physical properties of ice with significant admixed debris (e.g. Arenson & Springman 2005a, 2005b) (Fig. 15). For example, comparing the coefficient of thermal expansion, α , employed in our simple model of ice fracture ($5 \times 10^{-5} \text{ K}^{-1}$) to reasonable coefficients of thermal expansion for basalt (comparable in composition to the dolerite till covering Mullins and Beacon valleys), $6\text{--}8 \times 10^{-6} \text{ K}^{-1}$ (Touloukian *et al.* 1981), it becomes apparent that an ice-till mixture will have a significantly different bulk coefficient of thermal expansion due to the presence of low- α mineral grains. Lowering the coefficient of thermal expansion of trough-filling material reduces the tensile stress resulting from cooling. In this manner, although the polygon trough is materially weaker than the surrounding ice due to the presence of a crack, a filled trough may reduce thermal stresses associated with temperature change by virtue of experiencing diminished thermal contraction. Further, overlying snow, trapped preferentially in deep polygon troughs, may insulate underlying ice from marked thermal variation (Marchant *et al.* 2002).

In summary, based on surface morphology, ice flow rates, preliminary cosmogenic nuclide exposure ages, and stress analyses, we conclude that the most likely explanation for variation in polygon morphologies observed in Mullins and central Beacon valleys is a model which combines initial thermal contraction crack formation radial to glacial flow in areas of relatively rapid ice flow velocities (i.e., oriented stress field), modified over ky-timescales by sublimation and deformation associated with glacial flow, and ultimately dominated by non-oriented thermal contraction in areas of stagnant buried ice. The inferred chronology for polygons in this system afforded by measured glacier flow

velocities and cosmogenic exposure ages on surface boulders suggests that some active polygons may have first formed as long as $\sim 600\,000$ years ago. Detailed analysis of subsurface temperature variation over time and space will permit refined modelling of crack generation and propagation due to thermal stresses in zones of ice stagnation (e.g. Kowalewski *et al.* 2006). Enhanced modeling of glacier thickness and flow rates will likewise improve our ability to model structural deformation in up-valley ice, improving our ability to determine the effects of glacier flow on polygon deformation.

Acknowledgements

This research was funded in part by NSF grant OPP-0338291. Also, the authors wish to acknowledge Douglas Kowalewski, Rebecca Parsons, Kate Swanger, and David Shean for field assistance, photographic support, and data support. High-resolution Cambot images were provided by the Airborne Topographic Mapper lab at the NASA Wallops Flight Facility. Finally, the authors would like to thank the referees, Nicholas Mangold, Chris McKay, John (Jack) Schroder, and Brian Whalley for their constructive reviews.

References

- ABRAMENKO, O.N. & KUZMIN, R.O. 2004. Presence of the two-generation polygonal net within impact craters on high latitudes of Mars. *Abstracts of the 40th Brown-Vernadsky Microsymposium*, Moscow.
- ARENSON, L.U. & SPRINGMAN, S.M. 2005a. Triaxial constant stress and constant strain rate tests on ice-rich permafrost samples. *Canadian Geotechnical Journal*, **42**, 412–430.
- ARENSON, L.U. & SPRINGMAN, S.M. 2005b. Mathematical descriptions for the behavior of ice-rich frozen soils at temperatures close to 0°C . *Canadian Geotechnical Journal*, **42**, 431–442.
- DORAN, P.T., DANA, G.L., HASTINGS, J.T. & WHARTON JR, R.A. 1995. McMurdo Dry Valleys Long-Term Ecological Research (LTER): LTER automatic weather network (LAWN). *Antarctic Journal of the United States*, **30**, 276–280.
- HOBBS, P.V. 1974. *Ice physics*. Oxford: Clarendon Press, 837 pp.
- KOWALEWSKI, D.E., MARCHANT, D.R., LEVY, J.S. & HEAD, J.W. 2006. Quantifying low rates of summertime sublimation for buried glacier ice in Beacon Valley, Antarctica. *Antarctic Science*, **18**, 421–428.
- LACHENBRUCH, A.H. 1962. Mechanics of thermal contraction cracks and ice-wedge polygons in permafrost. *Geological Society of America Special Papers*, **70**, 1–69.
- LORREY, A.M. 2002. *Distribution of patterned ground and surficial deposits on a debris-covered glacier surface in Mullins Valley and upper Beacon Valley, Antarctica*. Masters thesis, University of Maine, 126 pp.
- MANGOLD, N. 2005. High latitude patterned grounds on Mars: classification, distribution, and climatic control. *Icarus*, **174**, 336–359.
- MARCHANT, D.R. & HEAD, J.W. 2004. Microclimate zones in the Dry Valleys of Antarctica: implications for landscape evolution and climate change on Mars. *35th Lunar and Planetary Science Conference*, League City, TX.
- MARCHANT, D.R., LEWIS, A.R., PHILLIPS, W.M., MOORE, E.J., SOUCHEZ, R.A., DEONTON, G.H., SUGDEN, D.E., POTTER JR, N. & LANDIS, G.P. 2002. Formation of patterned ground and sublimation till over Miocene glacier ice in Beacon Valley, southern Victoria Land, Antarctica. *Geological Society of America Bulletin*, **114**, 718–730.

- MARCHANT, D.R., DENTON, G.H., SWISHER III, C.C. & POTTER JR, N. 1996. Late Cenozoic Antarctic paleoclimate reconstructed from volcanic ashes in the Dry Valleys region, south Victoria Land. *Geological Society of America Bulletin*, **108**, 181–194.
- MCCALL, J.G. 1960. The flow characteristics of a cirque glacier and their effect on glacial structure and cirque formation. In LEWIS, V.W., ed. *Norwegian Cirque Glacier*. London: The Royal Geographic Society Research Series, 39–62.
- MELLON, M.T. 1997. Small-scale polygonal features on Mars: seasonal thermal contraction cracks in permafrost. *Journal of Geophysical Research*, **102**, 25 617–25 628.
- PÉWÉ, T.L. 1974. Geomorphic processes in polar deserts. In SMILEY, T.L. & ZUMBERGE, J.H., eds. *Polar deserts and modern man*. Tucson: University of Arizona Press. 173 pp.
- PLUG, L.J. & WERNER, B.T. 2002. Non-linear dynamics of ice-wedge networks and resulting sensitivity to severe cooling events. *Nature*, **417**, 929–933.
- RIGNOT, E., HALLET, B. & FOUNTAIN, A. 2002. Rock glacier surface motion in Beacon Valley, Antarctica, from synthetic-aperture radar interferometry. *Geophysical Research Letters*, **29**, doi:10.1029/2001GL013494.
- SCHAEFER, J.M., IVY-OCHS, S., WIELER, R., LEYA, I., BAUER, H. & DENTON, G.H. 2000. Cosmogenic noble gas studies in the oldest landscape on Earth: surface exposure ages of the Dry valleys, Antarctica. *Earth and Planetary Science Letters*, **167**, 215–226.
- SCHAEFER, J.M., SHLUECHTER, C., WIELER, R., IVY-OCHS, S., KUBIK, P., MARCHANT, D., KORSCHINEK, G., KINE, K., HERZOG, G. & SEREFIDDIN, F. 2005. News from the oldest ice on Earth buried in Antarctica, and a new cosmogenic tool. *Geochimica et Cosmochimica Acta Supplement*, **69**, Supplement 1 (Goldschmidt Conference Abstracts 2005, A164).
- SCHWERTFEGER, W. 1984. *Weather and climate of the Antarctic*. Amsterdam: Elsevier, 327 pp.
- SLETTEN, R.S., HALLET, B., & FLETCHER, R.C. 2003. Resurfacing time of terrestrial surfaces by the formation and maturation of polygonally patterned ground. *Journal of Geophysical Research*, **108**, doi:10.1029/2002JE001914.
- SUGDEN, D.E., MARCHANT, D.R., POTTER JR, N., SOUCHEZ, R.A., DENTON, G.H., SWISHER III, C.C. & TISON, J. 1995. Preservation of Miocene glacier ice in East Antarctica. *Nature*, **376**, 412–414.
- TOULOUKIAN, Y.S., JUDD, W.R., AND ROY, R.F. 1981. *Physical properties of rocks and minerals*. New York: McGraw-Hill Book Company, 548 pp.

